# PROCEEDINGS OF SPIE

# Non-planar illumination sources for deflectometry

Quach, Henry, Kang, Hyukmo, Choi, Heejoo, Kim, Dae Wook

**SPIE.**

# Non-Planar Illumination Sources for Deflectometry

Henry Quach[a], Hyukmo Kang[a], Heejoo Choi[a,b], Dae Wook Kim[a,b,c,*]

[a]Wyant College of Optical Sciences, University of Arizona, 1630 E. University Blvd., Tucson, AZ 85721, USA
[b]Large Binocular Telescope Observatory, University of Arizona 933 N Cherry Avenue, Tucson, AZ 85721, USA
[c]Department of Astronomy and Steward Observatory, University of Arizona, 933 N. Cherry Ave., Tucson, AZ 85721, USA

## ABSTRACT

We introduce the design of a highly compact, non-planar illumination source for deflectometry. The source emits uniform and Lambertian light from a curved area resembling the inner bore of a cylinder. When equipped with motion hardware, the ring source behaves like a spatially modulated screen with a pixel pitch comparable to that of a typical LCD monitor. If this source, a detector, and test optic are coaxially aligned, then on-axis deflectometry measurements are possible for axicons and centrally obscured, convex optics. This paper highlights the illumination design behind a cylindrical ring source and its implementation as a prototype in the visible spectrum.

**Keywords:** Deflectometry, Convex Optics, Ray Recirculation

## 1. INTRODUCTION

During optical fabrication, in-situ metrology is highly desirable because it enables surface shape to be frequently measured without the time and accuracy penalties incurred during remounting and alignment. Null solutions such as in-situ interferometers exist; however, the cost of multiple null references to measure and guide a continuously evolving workpiece can be high. Alternatively, deflectometry has been shown to provide surface reconstruction accuracy similar to interferometry, particularly in the last decade.[1,2] A deflectometer uses a spatially well-defined source to illuminate a specular UUT, or unit under test. By using a camera to observe the light reflected at the UUT surface into the camera, the corresponding points between the light source, UUT surface, and detector that satisfy the law of reflection can be disambiguated. These correspondences are used to compute surface normal vectors at each UUT point, which are converted into surface slopes and integrated into surface shape.

An on-machine deflectometer is highly desirable because it can measure a wide range of manufactured optics in-situ. However, special attention must be given to the steepness and convexity of the desired UUTs. If a ray is traced in reverse from a detector pixel to an optical surface, the law of specular reflection implies that steeper slopes will deflect that ray more sharply than will gentler ones. If the surface is convex, the collection of these reverse-traced rays is generally deflected away from the surface's optical axis rather than towards it. Since steep and convex optics require the largest illumination sources, it is challenging and sometimes even impossible to configure a deflectometry system for full aperture measurement using exclusively *planar* sources within a manufacturing environment.

## 2. NON-PLANAR ILLUMINATION SOURCE MODELING

### 2.1 Non-Planar Deflectometry Source

If the emitting source is not bound to a plane and has freedom to surround a test surface, the source area required to perform a deflectometry measurement can be reduced. For instance, Figure 1 demonstrates the required sizes of two uniform and Lambertian sources to illuminate a horizontal stripe across a steep cylindrical UUT.
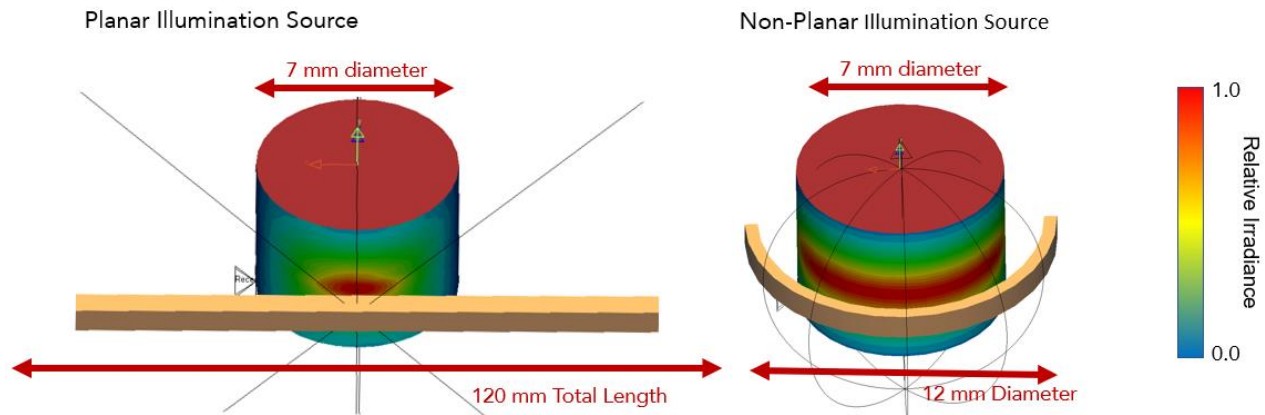
* letter2dwk@hotmail.com

Figure 1. A 7 mm diameter cylinder is illuminated by two uniform and Lambertian sources of equal radiance in LightTools. The length of the planar source (left) must be more than ten times the cylinder diameter in order to illuminate the periphery of the horizon to at least one third of the irradiance at the center. This nonuniformity is due to the irradiance falloff with source-to-target distance and the diminishing projected solid angle between further differential source areas and the target area. If a concave emissive strip (right) wraps around the cylinder instead, the same horizon can be illuminated with much greater uniformity. The nonuniform irradiance from planar illumination arises mostly for steep or convex surfaces and is less pronounced for flatter ones.

The impact of highly nonuniform irradiance at the UUT surface on deflectometry measurement is clear when one adjusts the exposure of the acquisition camera. For the left case, tuning the exposure effectively optimizes for maximum unsaturated brightness at the pixels viewing the cylinder vertex because in this illumination scenario, the vertex region naturally has the highest incident flux. At this set exposure value, the pixels viewing the periphery consequently suffer from limited maximum brightness and contrast. Whether using a weighting algorithm or Gaussian fitting to perform the deflectometry calculation, lower contrast at any pixel decreases overall measurement precision.[3,4]

Since curved sources can illuminate the aperture of a highly sloped test optic without the substantial irradiance falloff seen from planar sources, customizing sources to test specific types of optics without substantial loss of precision becomes an interesting possibility. Curved LCD screens are now commercially available, but they are limited to the visible spectrum and mostly to larger curvatures. A cylindrical source architecture that is customizable for curvature and applicable across multiple wavelengths is now proposed.

## 2.2 Non-Sequential Illumination Design of a Cylindrical Ring Source

Graves introduced the use of a rectangular integrating box architecture to create a high-contrast LWIR source for infrared deflectometry.[5] Instead of heating a metal ribbon, numerous modular LWIR sources are placed into a machined aluminum cavity. Rays diffusely reflect between the roughened interior walls until their position and angle fit within the spatio-angular envelope required to escape the cavity. The result is a relatively uniform and Lambertian distribution at the exit slit.

Adopting this architecture, an annular cavity with an interior cylindrical exit slit (2 mm in width and 90 mm in diameter) was designed. The goal is to obtain a uniform, Lambertian radiance distribution for a ring of input light sources within the cavity. A cylindrical receiver is defined at the exit of the cavity, with azimuthal coordinates, $\theta$, and height coordinate, $z$. Some guidelines based on the cavity design literature and many non-sequential raytracing simulations were invoked, resulting in the form factor seen in Figure 2.

1. Cavity walls are designed to be diffuse and parallel to obtain higher uniformity across the cylindrical receiver area. To achieve better spatial integration, both stable and unstable cavity geometries from the laser physics literature were explored.[6] LightTools simulations of combinations of concave, convex, and flat walls show that a cavity consisting of pairs of parallel walls of similar curvature is helpful towards high spatial integration of initial distributions.
2. A 'serial chamber' design is used to obtain a more Lambertian intensity distribution. If only a single chamber is used to integrate light, the output intensity distribution is askew, or preferentially emits downwards rather than centered on the horizontal plane defining the exit slit. To achieve intensity distribution symmetry across the vertical direction, a narrow second upper chamber/tunnel follows the first, with the open wall defining the overall exit slit of the cavity.

3. Since uniformity and intensity objectives ire already reasonably satisfied, the overall interior volume and surface area are decreased to increase the amount of radiance available at the cavity walls. In an integrating sphere, decreasing the volume increases flux at the exit port at the cost of some spatial integration performance.[7]
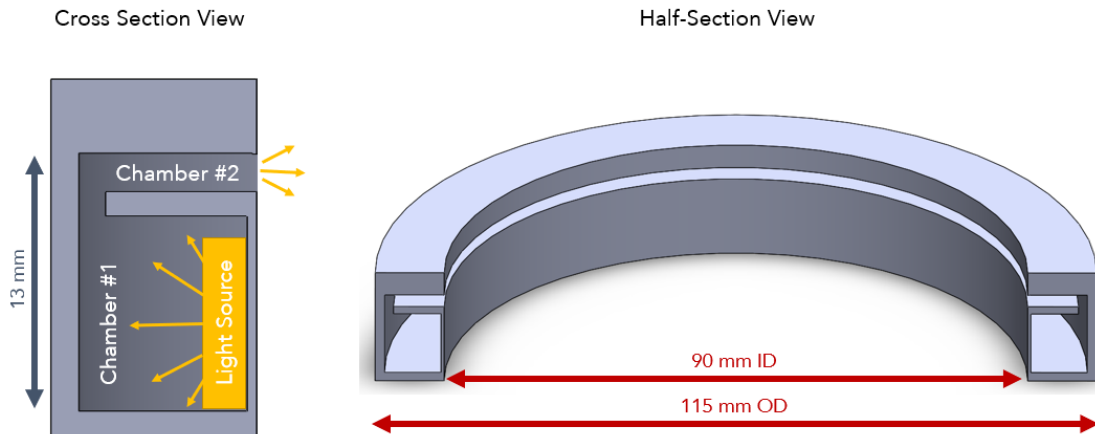


Figure 2. The system was first conceptually designed as a model in SolidWorks. The design was parametrically modeled in LightTools, where parameters such as wall thickness or flange length could be optimized for output uniformity or total flux at the receiver. The cross section (left) of the revolved surface (right) illustrates the form of the integrating chambers. A ring of light sources (i.e. LEDs, modular emitters) faces the opposite direction of the exit slit. This generic form can be scaled in diameter and the number of input sources to obtain the desired distribution for a given wavelength.

To complete the modeling, a design wavelength, light source, and material properties were assigned. Since the source was designed with the intent to be built, choosing to implement the source in the visible wavelength output was practical due to the limited hardware outside of lab during the COVID-19 pandemic. The selected LEDs each had a 120° FOV and were contained within the standard 3528 form factor (3.5 mm x 2.8 mm). In this model, 95% material reflectance and low order cosine scattering characterized ray behavior and absorptive loss at reflection. After optimization, the relatively uniform and Lambertian radiance distribution was achieved and is shown in Figure 3.
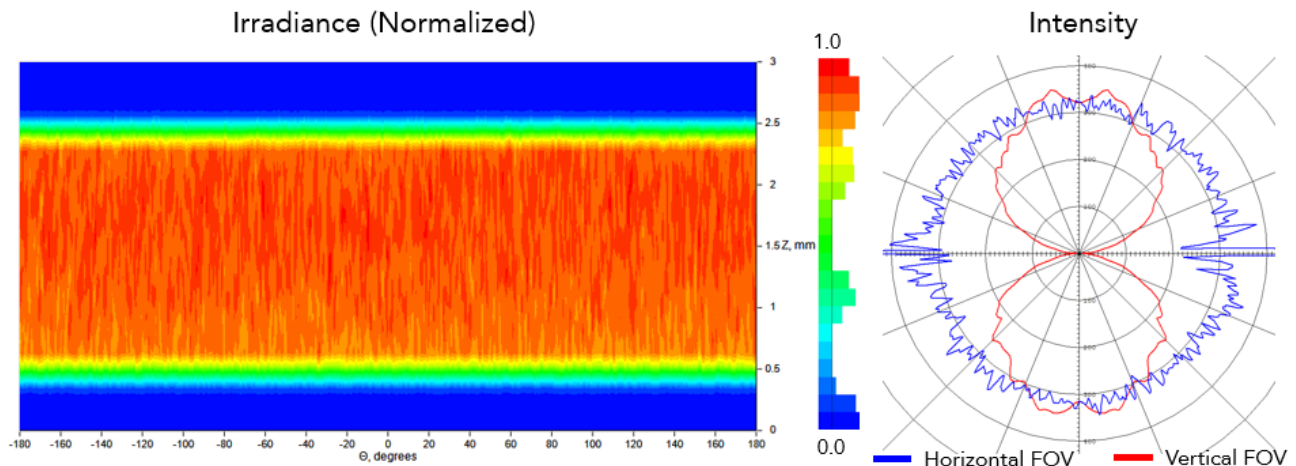


Figure 3. Sampling 10 million rays from 36 small LEDs within the cavity, non-sequential ray tracing simulation demonstrated a flux efficiency of 18.3% (input flux over output flux). The irradiance distribution plot is mapped over a cylindrical coordinate system, showing the relatively high uniformity across the full unwrapped azimuth with 6% average error at the least irradiated receiver pixel. Irradiance was highly consistent over the 2 mm vertical exit dimension, and overall the average deviation (standard deviation normalized with respect to maximum irradiance across the mesh) was 0.138. The line charts show that intensity across the horizontal direction (blue) is similar across all direction, as expected from the symmetry of the system, with 14% average error at the least irriadiated receiver pixel. In the vertical direcion (red), nearly Lambertian behavior is observed. Note that a mirrored vertical distribution exists as a consequence of 'inwards' light propagation within the cylindrical system.

## 2.3 Temporal Light Modulation Scheme

To modulate the light across the uniform ring source (as required to perform deflectometry), motion-controlled vertical movement and azimuthal masking are used. Since the entire assembly is so small and compact, it can be easily fixed to a commercial external translation stage for scanning along a UUT's optical axis. To achieve this motion in-situ, the cavity can also be directly mounted to linear motion DOFs already built into an optic CNC machine. Movement of the source in this linear direction can disambiguate the position, $z$, along the optical axis that satisfies the law of reflection between points at the UUT and the source.

For azimuthal motion, a binary mask is placed directly atop and concentric to the rest of the cylindrical cavity. The cylindrical mask has a slit subtending a small angle from the center of curvature and is rotated to select the azimuth of permitted light emission. Implementing rotation of this mask is mechanically interesting because power transmission cannot begin at the cavity's center, which must remain unobscured. One solution is to integrate gear teeth at the outer perimeter of the mask. A nearby smaller pinion, fixed to a stepper motor, meshes with these integrated gear teeth, so that the azimuth of light emission can be digitally controlled. Movement of the source in this direction can disambiguate the azimuth angle, $\theta$, around the optical axis that satisfies the law of reflection between points at the UUT and the source.

As the radius of the concentric cavity, $\rho$, is fixed, we have obtained a cylindrical screen whose positions are specified by $(\rho, \theta, z)$. Standard linear motion hardware can obtain tens of microns of precision and standard stepper motors can easily be driven at 2000 microsteps per revolution without precision loss due to insufficient torque. Thus the 'pixel 'pitch' of the screen for the described source is in the hundreds of microns range without specialty hardware. Note that the calculated pixel pitch does not limit the resolution of measurement; subpixel resolution is obtained by weighted averaging or fitting the specular response signal of the discrete sampled measurements.

# 3.   VISIBLE RING SOURCE PROTOTYPE

## 3.1 Integrating Cavity Construction

The illumination design model was adapted to a mechanical prototype with 3D printed parts shown in Figure 4. The top-level prototype can be visualized as into a reflective white integrating cavity subassembly and an absorptive black housing subassembly to suppress stray light. Due to the iterative nature of prototyping, each subassembly was further split into multiple components for efficient design changes. The light source procured was a continuous strip of 36 LEDs (Model #CB-62K) from the FlexFire LEDS. This manufacturer was chosen because their LEDs are binned before assembly and the availability of a 24V power option meant better thermal performance and component lifetime.
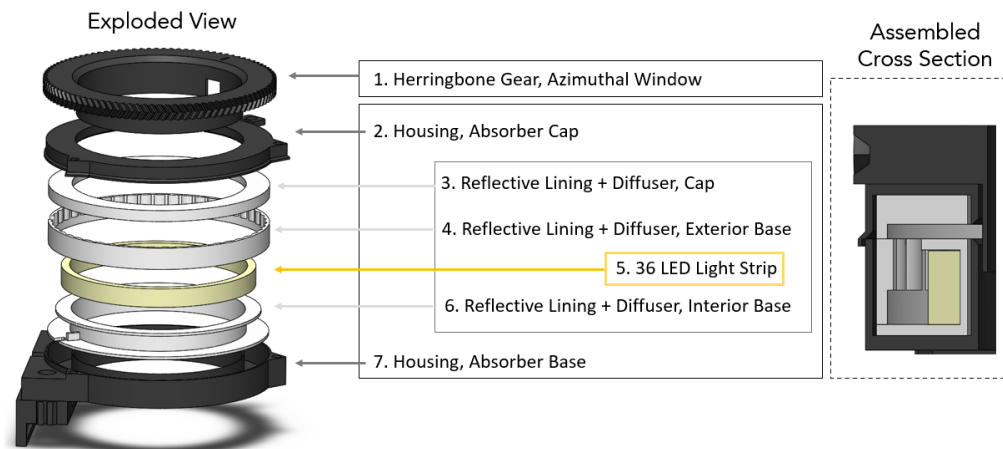


Figure 4. The nested layer design simply allows greatly flexibility for rapid prototyping. Instead of a monolithic cavity that had to be fully reprinted between iterations, changes to the walls could be done piecemeal to enable faster performance evaluation. Layer 1, the azimuthal window, is concentric to the Layer 2-7 illumination ring assembly. A 96-tooth herringbone gear is driven by a 32-tooth herringbone pinion, affixed to a stepper motor shaft. The interior volume (between layers 3-6) was minimized as to maximize the output radiance at the exit slit. Layer 4 is the outer wall with steep cylindrical facets, which help diffuse the light along the azimuthal direction (this was not included in the illumination design mode but is included here nonetheless). The tolerance of these features is less important for a diffusing design.

Parts were printed with FFF (fused filament fabrication) from an Ultimaker 2+ with the black and white PLA plastic manufactured by Atomic Filament. The 3D-printed azimuthal binary mask was implemented by integrating herringbone gear teeth into the outer cylindrical side of the mask. Herringbone gears are a variation of a helical gear that do not produce an axial load and therefore relax bearing mounting and axial runout requirements. White plastic walls were sanded with 60 and 40 grit sandpaper as to increase surface roughness and eliminate the natural sheen of the 3D printed surfaces.

Simple and inexpensive, this source is completely 3D printed and was implemented with relatively inexpensive and accessible electronics. Figure 5 demonstrates some of the assembly process and the structure of the mounted cavity. In the future, a UUT and camera are to be added and aligned coaxial with the axis of the source.
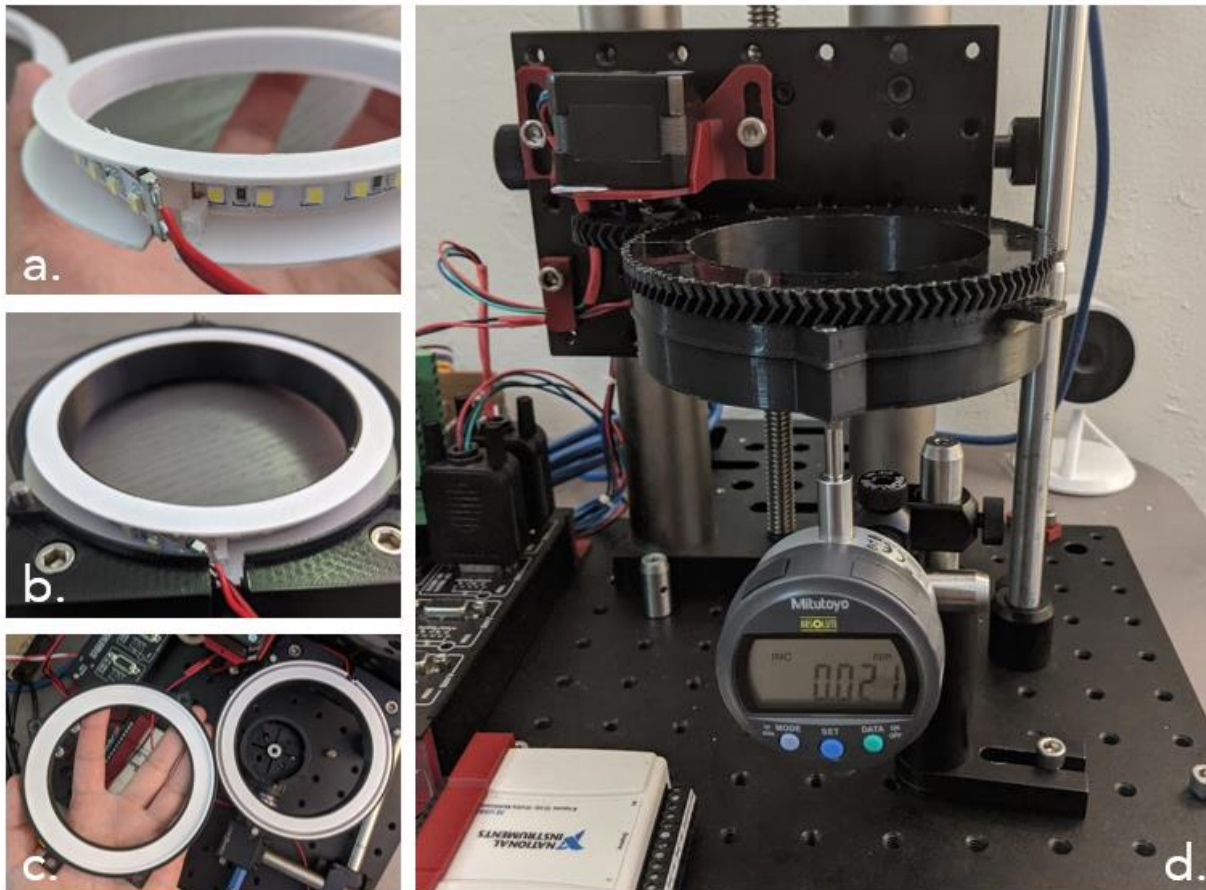


Figure 5. The base of the deflectometer was built by affixing two stepper motors to a Melles Griot vertical translation stage. A coupler was attached to the lead screw and grasped by a stepper motor to drive it. The second motor was mounted to its carriage and rotated a pinion to drive the 3D-printed herringbone gear at a 1:3 ratio. Both steppers are driven by a GeckoDrive G540 stepper motor driver and a National Instruments DAQ (Model USB-6008). Preliminary tests show that motion can be synchronized with a PointGrey Camera (Model FL3-U3-13Y3-C with a $f$ =16 mm Computar lens) such that snapshots with an exposure time of just 14 ms already achieve full pixel saturation, which reflects the intrinsic brightness of the source.

## 4.  CONCLUSIONS

We demonstrate the implementation of a customized visible light source for on-axis deflectometer that is suited to measure highly convex shapes within a highly confined volume. The full assembly was 3D printed and integrated with commercial electronics and drivers inside a student's home during the COVID-19 global pandemic. The illumination design was built in a modular architecture for rapid prototyping and a fully automated image acquisition system was created. More work is to be done to understand to verify reconstruction accuracy for a convex UUT with a central obscuration as well as to identify the limitations of the mechanically-driven cylindrical ring source.

## ACKNOWLEDGEMENTS

## REFERENCES

[1]    Huang, L., Idir, M., Zuo, C. and Asundi, A., "Review of phase measuring deflectometry," Opt. Lasers Eng. **107**(August), 247–257 (2018).

[2]    Zhang, Z., Wang, Y., Huang, S., Liu, Y., Chang, C., Gao, F. and Jiang, X., "Three-Dimensional Shape Measurements of Specular Objects Using Phase-Measuring Deflectometry," Sensors **17**(2835) (2017).

[3]    Su, T., Park, W. H., Parks, R. E., Su, P. and Burge, J. H., "Scanning Long-wave Optical Test System: a new ground optical surface slope test system," Opt. Manuf. Test. IX **8126**(May), 81260E (2011).

[4]    Lowman, A. E., Yoo, H., Smith, G. A., Oh, C. J. and Dubin, M., "Improvements in the scanning long-wave optical test system," 48 (2018).

[5]    Graves, L. R., Quach, H., Koshel, R. J., Oh, C.-J. and Kim, D. W., "High contrast thermal deflectometry using long-wave infrared time modulated integrating cavity source," Opt. Express **27**(20), 28660 (2019).

[6]    Milonni, P. W. and Eberly, J. H., [Laser Physics, 1st ed.], John Wiley & Sons, Inc., Hoboken, New Jersey (2010).

[7]    Labsphere., "Integrating Sphere Theory and Applications" (2017).